Thermochimica Acta 494 (2009) 104–109

Contents lists available at ScienceDirect

Thermochimica Acta

journal homepage: www.elsevier.com/locate/tca

Formaldehyde-free and thermal resistant microcapsules containing *n*-octadecane

X.L. Shan, J.P. Wang, X.X. Zhang*, X.C. Wang

Tianjin Municipal Key Lab of Modification and Functional Fibers, Tianjin Polytechnic University, Tianjin 300160, PR China

ARTICLE INFO

Article history:
Received 2 March 2009
Received in revised form 28 April 2009
Accepted 30 April 2009
Available online 15 May 2009

Keywords:
Microencapsulation
n-Octadecane
Thermal resistant temperature
Formaldehyde-free

ABSTRACT

Microcapsules containing *n*-octadecane were synthesized using methacrylic acid (MAA), methyl methacrylate (MMA) and 1,4-butylene glycol diacrylate (BDDA) as shell. The surface morphology, thermal physical properties, thermal stabilities and diameter distributions of the microcapsules were investigated using scanning electron microscopy (SEM), differential scanning calorimetry (DSC), thermogravimetric analysis (TG) and particle size distribution analysis, respectively. The experimental results show that, the core material is well encapsulated in the presence of emulsifier—sodium salt of styrene–maleic anhydride co-polymer. The average diameter of the microcapsules is 18 μm. The enthalpy of microencapsulated *n*-octadecane (MC_{18}) with MAA–MMA co-polymeric shell is 155 J g^{-1} which corresponds to 70 wt.% core content. The thermal resistant temperature of MC_{18} is 238 °C, which is affected by *n*-octadecane/monomers mass ratios and the content of cross-linking agent-BDDA.

1. Introduction

Microcapsules are tiny particles that contain active agent or core material surrounded by a coating or shell [1]. Phase change materials, i.e. water, *n*-octadecane, polyethylene glycol, butyl stearate, calcium chloride hexahydrate, etc. can absorb or release 150–334 J g^{-1} of latent heat [2]. Microencapsulated phase change materials (MicroPCMs) have been considered as renewable and clean energy storage materials since 1980s. They can absorb and release heat reversible without producing any wastes [3]. MicroPCMs have been attempted widely to be used in the manufacture of building materials [2], thermo-regulated fibers [4], fabrics [5], foams [6], coatings [7], etc. since then; and MicroPCMs have been used as wallboard, ceiling or coolant in energy saving building [2]. MicroPCMs absorb heat from the atmosphere during daytime and release the heat during nighttime. The applications of PCM wallboard as a load management device for passive solar applications were found to save energy with reasonable pay back time periods [2].

Melamine–formaldehyde (MF) resin has been widely used as shell material of microcapsule since its low price, high mechanical strength [8,9]. Up till now, there are more than a half of attempts using MF resin as shell material to fabricate MicroPCMs, in which formaldehyde was a necessary reactant [10–12]. As we all have known, formaldehyde is a kind of toxic and irritating substance which causes environmental and health problems. Although excess formaldehyde can be reduced by using some efficient methods as has been reported in our previous research, residual formaldehyde was still present in the wall of the microcapsules [13]. MicroPCMs with formaldehyde-free polymer shell, such as polyurea [14–16], polyurethane–urea [17] and silica formed by the hydrolysis, condensation of tetraethyl silicate [18], etc. have been developed. Some of them have an unstable reaction process and a lower microencapsulated efficiency (ratio of measured enthalpy of MicroPCMs and theoretical enthalpy calculated according to the raw materials) than that of MF [14], however. Furthermore, in some special environments, particular high thermal resistance of MicroPCMs is crucial for the application, i.e. the melt-spun thermo-regulated fibers [19], the coating for stealth of an airplane to infrared detection [7], etc. MicroPCMs have to undergo a high temperature process during the lift and landing process of a nose-dive airplane. Therefore, the microcapsules with high thermal resistance are required for the application.

Microcapsules using acrylic co-polymer as shell were reported by Ciba, however, there is little information available about their structure and properties. Microcapsules with acrylic co-polymeric shell containing phase change materials were prepared in this paper. MicroPCMs with poly(MAA–MMA) and poly(BDDA–MAA–MMA) co-polymer shell were obtained, respectively, attempt to obtain microcapsules which are formaldehyde-free and high temperature resistance.

2. Experimental

2.1. Materials

MAA and MMA (purity 90 wt.% and 99.5 wt.%, Tianjin Kermel Chemical Reagent Co., Ltd.) were used as shell-forming monomers.

* Corresponding author. Tel.: +86 22 24528144; fax: +86 22 24348894.
E-mail address: zhangpolyu@yahoo.com.cn (X.X. Zhang).

0040-6031/$ – see front matter © 2009 Elsevier B.V. All rights reserved.
doi:10.1016/j.tca.2009.04.026

1,4-Butanediol diacrylate (BDDA, purity 98.5 wt.%, Shanghai Kangming Chemical Reagent Co., Ltd.) was used as cross-linking agent. MAA was purified by vacuum distillation. MMA was washed with 5 wt.% sodium hydroxide aqueous solution to remove the inhibitor-Bisphenol A; and dried in $CaCl_2$ overnight. *n*-Octadecane (purity 95 wt.%, Union Lab. Supplies Limited, Hong Kong) was used as core material. Benzoyl peroxide (BPO, purity 99 wt.%, Tianjin Chemical Reagent Co., Ltd.) was used as an initiator. Sodium salt emulsion of styrene–maleic anhydride co-polymer (SMA, 19 wt.% aqueous solutions, Shanghai Leather Chemical Works) was employed as an emulsifier. Potassium persulphate (A.R., Tianjin Chemical Reagent Co., Ltd.) was added into the initial resultant mixture as a secondary initiator.

2.2. Fabrication of MC_{18}

Microencapsulation was carried out in a 250 ml three-neck round-bottomed flask equipped with a mechanical stirrer, a reflux condenser and a nitrogen gas inlet tube. The flask was put in a water thermostat bath.

The polymerization system was consisted of an oil phase and a water phase. The oil phase was made up of *n*-octadecane, MAA, MMA and BPO, and the water phase was made of 10 g SMA and 100 g distilled water at 55 °C. The oil phase was added into the water phase by continuously stirring. The mixture was emulsified with a stirring rate of 1200 rpm or 1600 rpm for about 15 min to form a stable emulsion system. Then the temperature was raised to 75 °C and kept for 3 h with a stirring rate of 800 rpm. One-tenth gram of potassium persulphate was dissolved in 1.4 g of water to form an aqueous solution as a second initiator which was added into the reaction mixture and continued for 1.5 h with the same stirring rate. The resultant mixture was filtered and washed with distilled water at 50 °C to eliminate impurities (i.e. monomers, water soluble prepolymer, unencapsulated *n*-octadecane, emulsifier, etc.), and then the wet cake was dried in an oven at 50 °C for 48 h to remove the residual water. Powder-like products were obtained.

The fabrication process of MAA–MMA co-polymer as follows: 0.6 g SMA was dissolved in 100 g distilled water at 55 °C. The oil phase was composed of MAA, MMA and BPO. The amount of oil phase component (without PCM) and reaction condition were the same as the fabrication of MC_{18}. The reaction mixture was filtered and well washed with distilled water; the pure MAA–MMA co-polymer is produced.

To investigate the effect of cross-linking agent on the morphologies and properties of MicroPCMs, samples of MC_{18} with MAA–MMA–BDDA co-polymer as shell were prepared. Their fabrication process was almost the same as the ones with MAA–MMA binary co-polymer shell, except that the oil phase was made up of *n*-octadecane, MAA, MMA, BDDA and BPO. During the fabrication process, 0.1 g of potassium persulphate was dissolved in 1.4 g of water to form an aqueous solution which was also added as a second initiator. It is helpful for a small amount of co-monomers dissolving in the water phase to deposit on the shell.

The recipes used for the fabrication of MAA–MMA co-polymer and a series of MC_{18} without and with BDDA are presented in Table 1.

2.3. Characterization of MC_{18}

The surface morphologies of MC_{18} were examined by using a scanning electronic microscope (SEM, Quanta-200). A drop of the microcapsule suspension was dripped on a stainless steel SEM stub and air-dried overnight. Then the samples were gold-coated.

Spectra of *n*-octadecane, MAA–MMA co-polymer and MC_{18} were obtained using a Fourier transformed infrared spectroscopy (FTIR, Bruker Uecior-22, wave number 4000–400 cm^{-1}) at room temperature.

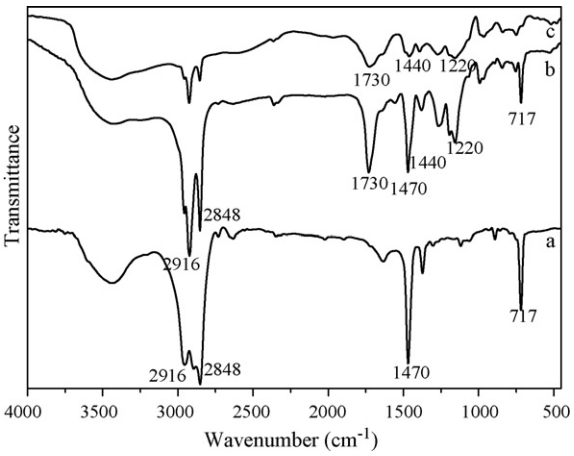

Fig. 1. FTIR spectra of *n*-octadecane, Sample No. 2 and MAA–MMA co-polymer ((a) *n*-octadecane; (b) Sample No. 2; (c) MAA–MMA co-polymer).

The thermal properties of MC_{18} were measured using a differential scanning calorimeter (DSC, PerkinElmer) in the range of 0–80 °C at a heating or cooling rate of ±10 °C min^{-1} in a nitrogen atmosphere. The content of *n*-octadecane in the microcapsules was calculated according to the measured enthalpies:

$$x = \frac{|\Delta H|}{|\Delta H_0|} \times 100\%$$

where x is the weight percentage content of *n*-octadecane; $|\Delta H|$ is the melting enthalpy of MC_{18}; $|\Delta H_0|$ is the melting enthalpy of *n*-octadecane.

The thermal resistance of MC_{18} was investigated by using a thermogravimetric analyzer (TGA, NETZSCH STA 409 PC/PG TG-DT) at a scanning rate of 10 °C min^{-1} in the range of 25–600 °C in a nitrogen atmosphere.

The diameter distribution of MC_{18} was examined by using a diameter distribution analyzer (HORIBA LA-300).

3. Results and discussion

3.1. Formation of MC_{18}

The FTIR spectra of *n*-octadecane, Sample No. 2 and MAA–MMA co-polymer are shown in Fig. 1.

The multiple strong absorption peaks locate at approximately 2848–2916 cm^{-1} and 717 cm^{-1} in the spectra of *n*-octadecane and the microcapsules are associated with the aliphatic C–H stretching vibration and the in-plane rocking vibration of the CH_2 group, respectively [21,22]. The peak at 1470 cm^{-1}, which is associated with the C–H bending, is also characteristic for *n*-octadecane. None of these specific peaks are observed in the spectrum of the polymer shell, however. In addition, some of the specific peaks are only found in the spectra of the polymer shell and Sample No. 2. For instance, the peak at about 1730 cm^{-1} is assigned to carbonyl group. The peak at 1220 cm^{-1} is assigned to C–O stretching of ester group in MMA [23]. These characterized peaks are observed in the spectrum of the microcapsules which indicate that *n*-octadecane as core has been successfully encapsulated by the shell of MAA–MMA co-polymer.

3.2. Surface morphology of MC_{18}

Fig. 2 shows SEM micrograph of Sample No. 2 fabricated with *n*-octadecane/monomers mass ratio of 2:1. The microcapsules are spherical particles with an average diameter of about 20 μm. There

Table 1
Recipes for the fabrication of MAA–MMA co-polymer, MC_{18}.

Sample No.	Water phase		Oil phase						*n*-Octadecane/ monomers (mass ratios)	Stirring rate (rpm)
	H_2O (g)	SMA (g)	MMA (g)	MAA (g)	BDDA (g)	*n*-Otadecane (g)	BPO (g)	$K_2S_2O_8$ (g)		
MAA–MMA co-polymer	100	0.6	3.7	1.9	0	0	0.2	0.1	–	1200
1	100	10	3.7	1.9	0	13	0.2	0.1	23:10	1200
2	100	10	3.7	1.9	0	11.5	0.2	0.1	2:1	1200
3	100	10	3.7	1.9	0	9.0	0.2	0.1	8:5	1200
4	100	10	3.7	1.9	0	5.6	0.2	0.1	1:1	1200
5	100	10	3.7	1.9	0.4	9.0	0.2	0.1	9:6	1200
6	100	10	3.7	1.9	0.2	5.6	0.2	0.1	28:29	1200

MAA, methacrylic acid; MMA, methyl methacrylate; BDDA, 1,4-butylene glycol diacrylate; BPO, benzoyl peroxide; SMA, sodium salt of styrene–maleic anhydride co-polymer.

are many dimples on all of the microcapsules. The morphology of the microcapsule is different from that of microcapsule using MF as shell [21,24]. There are many tiny particles attached on the surface of the microcapsule using MF as shell. These tiny particles are probably the MF polymer formed during polymerization failed to encapsulate *n*-octadecane. This can be explained by the difference of polymerization mechanism. The co-polymerization in this paper starts at the interface between the oil phase and the water phase. The monomers disperse from the oil phase to the interface and take part in the polymerization. The thickness of the shell increases continuously toward the inner of the microcapsule. The shell shrinks gradually during the co-polymerization process since the density of the co-polymer is higher than that of the monomer. By contrast, the MF shell is formed on the surface of oil sphere in *in-situ* polymerization using MF as shell by regulating pH of the emulsion [24]. Thickness of the shell increases continuously toward the outer of the microcapsule. The shell does not shrink during the fabrication process; and it only shrinks when the emulsion temperature decreases from polymerization temperature (i.e. 65 °C or 70 °C) to room temperature.

3.3. Effects of the stirring rate on diameters and their distribution of MC_{18}

Diameter distribution curves of MC_{18} using various stirring rates are presented in Fig. 3. The stirring rates during emulsion process were set as 1200 rpm and 1600 rpm for about 15 min, respectively. When the stirring rate in emulsion process is 1200 rpm, the diameters are in the range of 0.5–40 μm; and the average diameter is about 18 μm. By contrast, when it is increased to 1600 rpm, the diameters are in the range of 0.5–30 μm; and the average diameter is about 11 μm. As has been reported in the literature, the stirring rate is an important factor that affects the diameter and diameter distribution [21]. The diameter range of Sample No. 2 is narrowed from approximately 39.5 μm to 29.5 μm as the stirring rate increases from 1200 rpm to 1600 rpm. To some extent the faster

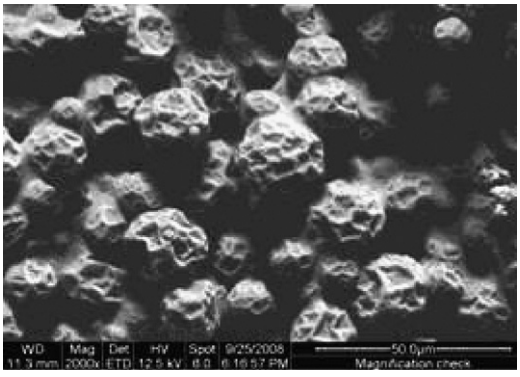

Fig. 2. SEM micrograph of Sample No. 2.

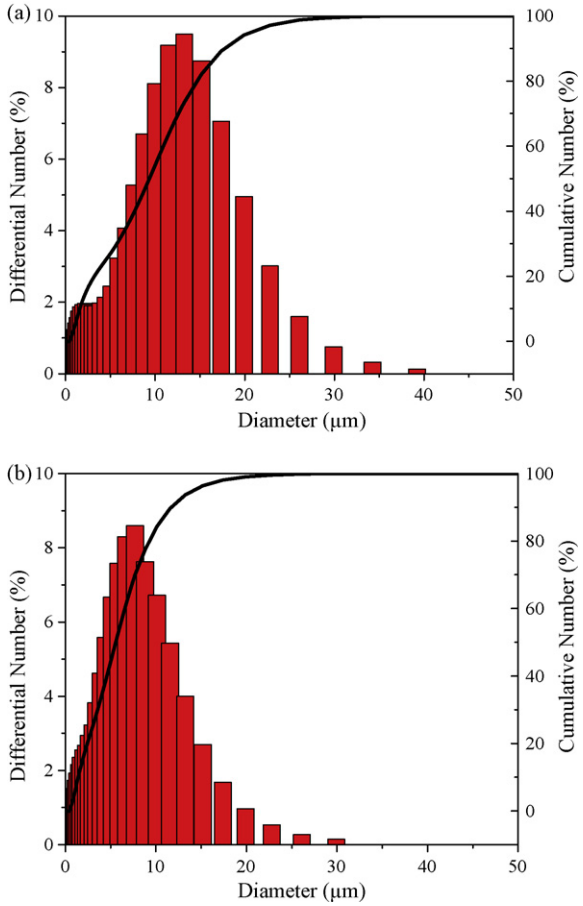

Fig. 3. Size distribution curves of Sample No. 2 ((a) 1200 rpm; (b) 1600 rpm).

of the stirring rate, the diameter is the smaller, and the diameter distribution is the narrower.

3.4. Phase change properties of MC_{18}

DSC curves of MAA–MMA co-polymer, *n*-octadecane and Sample No. 2 are presented in Fig. 4. Endothermic peak and exothermic peak in the process of heating and cooling of Sample No. 2 and *n*-octadecane are observed in the range of 0–80 °C while MAA–MMA co-polymer has none of them. During the endothermic process, the enthalpies of *n*-octadecane and Sample No. 2 are 222 J g^{-1} and 147 J g^{-1}; and the corresponding temperatures are 31 °C and 29 °C, respectively. The crystallizing temperature of *n*-octadecane inside microcapsule is approximately 5 °C lower than that of bulk *n*-octadecane. In addition, super cooling phenomenon is observed in the DSC cooling curve of Sample No. 2, which is resulted from the decrease of the number of nuclei with the reduction of diameter of

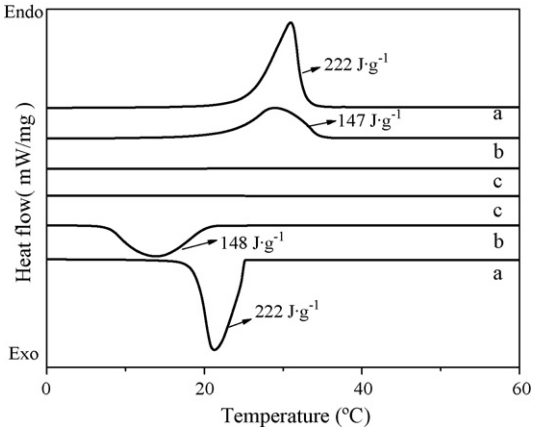

Fig. 4. DSC curves of samples ((a) *n*-octadecane; (b) Sample No. 2; (c) MAA–MMA co-polymer).

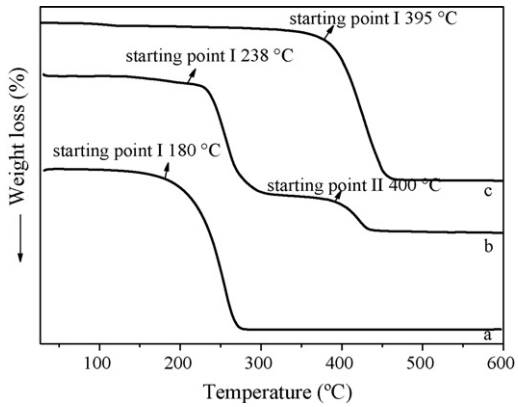

Fig. 5. TG curves of samples ((a) *n*-Octadecane; (b) Sample No. 2; (c) MAA–MMA co-polymer).

microcapsule [10,25]. Super cooling leads to the latent heat being released at a lower temperature, or in a wider temperature range. This effect limits the application of MicroPCMs [10].

3.5. Thermal resistance of MC_{18}

Fig. 5 shows TG curves of *n*-octadecane, MAA–MMA co-polymer and Sample No. 2. *n*-Octadecane starts to lose weight at nearly 180 °C, and loses weight completely at approximately 270 °C due to the evaporation before boiling point (308 °C) [13]. The weight-loss of MAA–MMA co-polymer at about 395 °C is caused by the decomposition of molecular chains. There is almost no weight-loss for Sample No. 2 under 238 °C. The weight-loss of Sample No. 2 above 238 °C is caused by the thermal expansion of core materials which diffuse out of shells in temperature rising process [11,24]. The second weight-loss temperature of Sample No. 2 is caused by the decomposition of MAA–MMA co-polymer. The thermal resistant temperature of Sample No. 2 with MAA–MMA co-polymer shell, which is defined as initial 5 wt.% weight-losing temperature in TG curve, is obviously higher than that of MC_{18} with MF shell [24]. The thermal resistant temperature of the latter is only approximately 152 °C. The acrylic co-polymer shell protects *n*-octadecane from losing weight quickly. The thermal resistant temperature of MC_{18} with MAA–MMA co-polymer shell is lower than that of MC_{18} with MF shell containing expansion space [11], however, that is due to the volume of expansion space inside the acrylic co-polymer shell being not high enough.

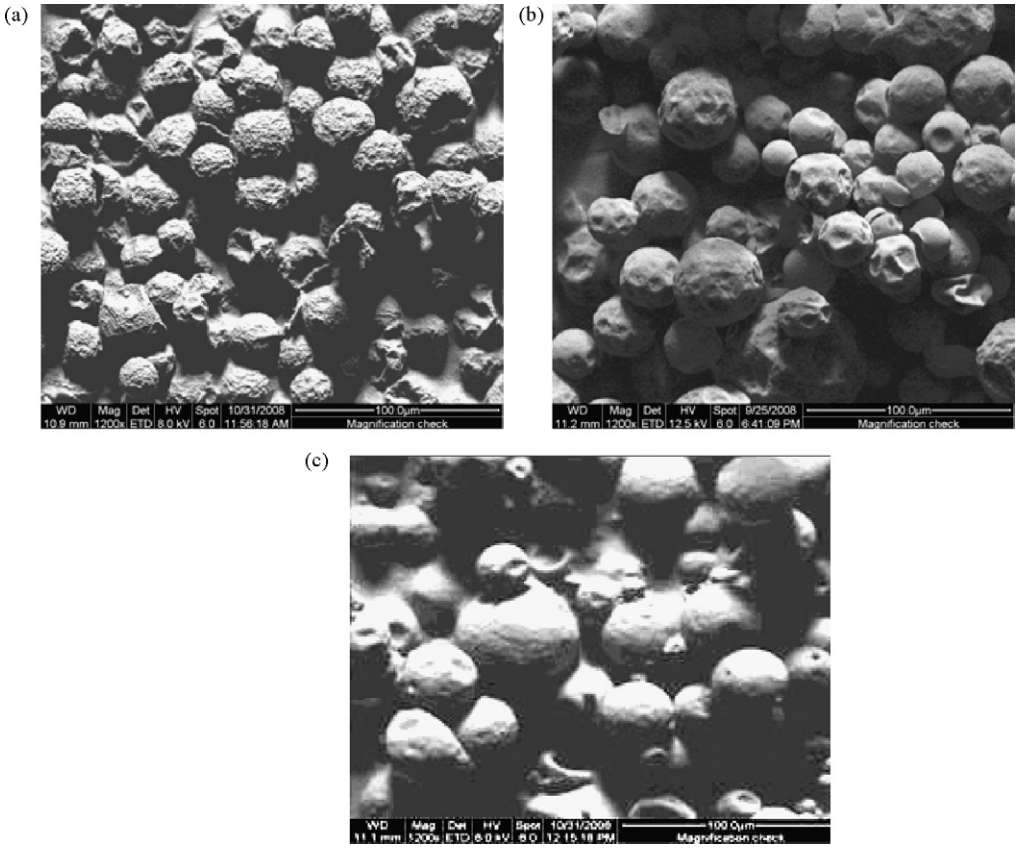

Fig. 6. SEM micrographs of MC_{18} with various contents of BDDA ((a) Sample No. 3 (BDDA 0%); (b) Sample No. 6 (BDDA 3.4%); (c) Sample No. 5 (BDDA 6.7%)].

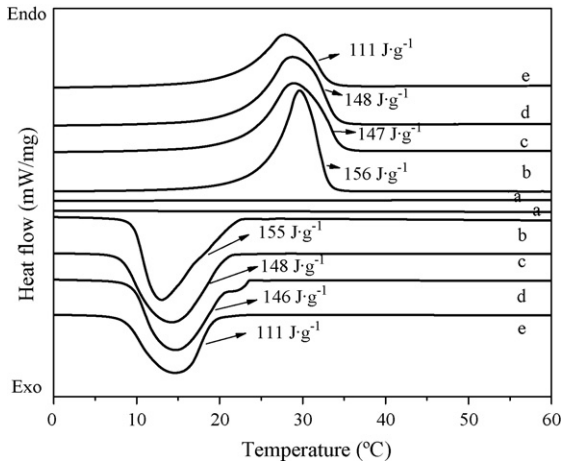

Fig. 7. DSC curves of MC_{18} with various *n*-octadecane/monomers mass ratios ((a) MAA–MMA co-polymer; (b) Sample No. 1; (c) Sample No. 2; (d) Sample No. 3; (e) Sample No. 4).

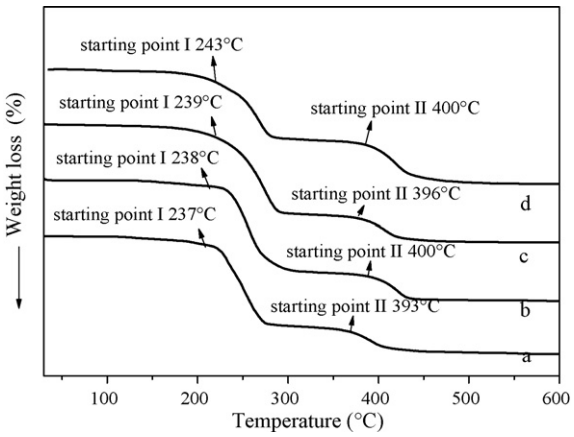

Fig. 8. TG curves of MC18 with various *n*-octadecane/monomers mass ratios ((a) Sample No. 1; (b) Sample No. 2; (c) Sample No. 3; (d) Sample No. 4).

3.6. Effects of the content of cross-linking agent on the morphology of MC_{18}

Fig. 6 shows SEM micrographs of MC_{18} fabricated with various contents of BDDA. The addition of cross-linking agent-BDDA makes the surfaces of microcapsules become smooth. The number of concaves existing on the surface of microcapsules decreases. The diameter of concave on the cross-linked shell increases, however. This may be explained as the degree of cross-links of co-polymer shell has been enhanced due to the addition of BDDA, and the higher the content of BDDA, the higher the degree of cross-link of shell materials in certain extent. The cross-linking increases the elastic modulus, the stress at the yield point, and the stress at break, and decreases the extension at break and the energy to break [26]. The concave on the shell, which is formed since the content of monomers decreases and the density of the co-polymer is higher than that of the monomer, is not easily formed when compared with that of without BDDA, however.

3.7. Effects of n-octadecane/monomers mass ratios on the enthalpy of MC_{18}

Fig. 7 shows DSC curves of MC_{18} with various *n*-octadecane/monomers mass ratios. The heat absorbing and evolving properties of MC_{18} are listed in Table 2. MC_{18} have both endothermic peak and exothermic peak in the process of heating and cooling in the range of 5–40 °C as they are compared with pure MAA–MMA co-polymer. The composition of various mass ratios has almost no effect on the melting temperature. Furthermore, when the *n*-octadecane/monomers mass ratio is 23:10, the enthalpy of MC_{18} is the highest, which corresponds to 70 wt.% of *n*-octadecane in the microcapsule. The enthalpy of MC_{18} decreases when *n*-octadecane/monomers mass ratio is less than 23:10 which corresponds to the decrease of PCM content.

3.8. Effects of n-octadecane/monomers mass ratios on the thermal resistance of MC_{18}

Fig. 8 shows the weight-loss percentages of MC_{18} with various mass ratios of MAA–MMA co-polymers. There are slight weight-loss under starting point I, which is caused by the evaporation of residual water and some not-reactive monomers and impurities. The thermal resistant temperature of MC_{18} enhances as the content of the shell increases. As the content of the shell increases, the thickness of the shell of every microcapsule increases. Therefore the strength of the shell is increased; and the core is not easy to diffuse out from the microcapsule [20].

3.9. Effects of the content of cross-linking agent on the thermal resistance of MC_{18}

The effects of the content of the cross-linking agent on the thermal resistance of MC_{18} are presented in Fig. 9.

The thermal resistance of MC_{18} is improved by adding the cross-linking agent. When the content of BDDA in the shell is low, the thermal resistance of MC_{18} do not increase significantly. It is enhanced obviously when the mass content of BDDA exceeds 5 wt.%. The thermal resistant temperature of the microcapsule containing 3.4 wt.% BDDA is 246 °C. The results also show that, the higher ~~of~~ the content of the cross-linking agent, the higher the thermal resistant temperatures of MC_{18} to a certain extent. The formation of cross-linked MAA–MMA–BDDA co-polymer strengthens the shell [26]. The thermal resistance of the shell is enhanced with the increase of the degree of cross-linking.

Table 2
Thermal properties of MC_{18} with various *n*-octadecane/monomers mass ratios.

Sample No.	*n*-Octadecane/monomers (mass ratios)	T_m (°C)	ΔH_m (J g^{-1})	T_c (°C)	ΔH_c (J g^{-1})	ΔH_a (J g^{-1})	*n*-Octadecane content (wt.%)
MAA–MMA co-polymer	0:1	–	0	–	0	0	
n-Octadecane	1:0	31	222	21	222	222	100
1	23:10	30	156	11	155	155.5	70
2	2:1	29	147	16	148	147.5	66.5
3	8:5	28	147	15	146	146.5	66
4	1:1	27	111	16	111	111	50

Note: T_m, melting point; ΔH_m, melting enthalpy; T_c, crystallization point; ΔH_c, crystallization enthalpy; $\Delta H_a = (|\Delta H_m| + |\Delta H_c|)/2$.

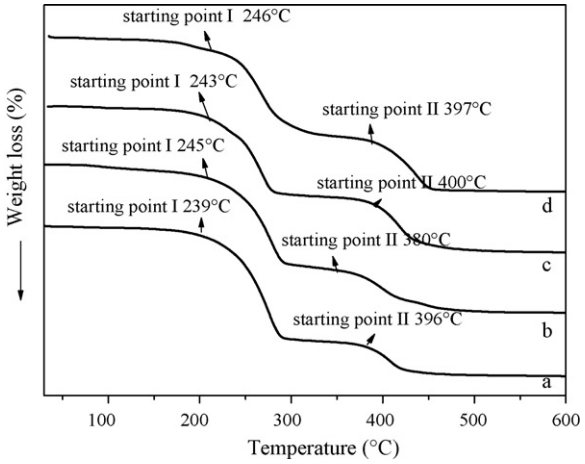

Fig. 9. TG curves of MC_{18} with various contents of cross-linking agent ((a) Sample No. 3 (BDDA 0%); (a) Sample No. 5 (BDDA 6.7%); (c) Sample No. 4 (BDDA 0%); (d) Sample No. 6 (BDDA 3.4%)].

4. Conclusions

Microencapsulated *n*-octadecane is fabricated by using methacrylic acid-methyl methacrylate-1,4-butylene glycol diacrylate co-polymer as shell material. The enthalpy of microencapsulated *n*-octadecane increases with increasing the content of *n*-octadecane in the core. The thermal resistant temperature of microencapsulated *n*-octadecane is above 238 °C. It is further enhanced with increasing the content of the shell due to the increase of shell thickness of every microcapsule. The thermal resistance of microencapsulated *n*-octadecane with methacrylic acid–methyl methacrylate co-polymer shell is remarkably improved by adding the cross-linking agent of 1,4-butylene glycol diacrylate. Especially when the content of co-monomer 1,4-butylene glycol diacrylate in the shell exceeds 5 wt.%, the thermal resistant temperature of microencapsulated *n*-octadecane is improved to 245 °C.

Acknowledgments

The authors are thankful to the National Natural Science Found of China (no. 50573058), Specialized Research Found for the Doctoral Program of Higher Education (no. 20050058004) and China Postdoctoral Science Foundation (no. 20070410764) for the financial supports.

References

[1] S. Benita, Microencapsulation: Methods and Industrial Applications, Marcel Dekker Inc., New York, 1996, pp. 1–3.
[2] A.M. Khudhair, M.M. Farid, Energy Convers. Manage. 45 (2004) 263–275.
[3] P.B.L. Chaurasia, Res. Ind. 26 (1981) 159–161.
[4] Y.G. Bryant, D.P. Colvin, US Patent 4756958 (1989).
[5] Y.G. Bryant, D.P. Colvin, WO9324241 (1993).
[6] M. You, X.X. Zhang, W. Li, X.C. Wang, Thermochim. Acta 472 (2008) 20–24.
[7] Y.G. Bryant, D.P. Colvin, J.C. Driscoll, J.C. Mulligan, CN1252025 (2000).
[8] G. Sun, Z. Zhang, J. Microencapsulation 18 (2001) 593–602.
[9] J.F. Su, L.X. Wang, L. Ren, Colloid Polym. Sci. 284 (2005) 224–228.
[10] X.X. Zhang, Y.F. Fan, X.M. Tao, K.L. Yick, J. Colloid Interface Sci. 281 (2005) 299–306.
[11] X.X. Zhang, X.M. Tao, K.L. Yick, Y.F. Fan, J. Appl. Polym. Sci. 97 (2005) 390–396.
[12] Y.F. Fan, X.X. Zhang, X.C. Wang, Q.B. Zhu, Thermochim. Acta 413 (2004) 1–6.
[13] W. Li, J.P. Wang, X.C. Wang, S.Z. Wu, X.X. Zhang, Colloid Polym. Sci. 285 (2007) 1691–1697.
[14] G.L. Zou, X.Z. Lan, Z.C. Tan, X. Sun, T. Zhang, Acta Phys. Chim. Sinica 20 (2004) 90–93.
[15] X.Z. Lan, Z.C. Tan, G.L. Zou, L.X. Sun, T. Zhang, Chin. J. Chem. 22 (2004) 411–414.
[16] X.Z. Lan, C.G. Yang, Z.C. Tan, L.X. Sun, F. Xu, Acta Phys. Chim. Sinica 23 (2007) 581–584.
[17] J.Y. Kwon, H.D. Kim, Fiber Polym. 7 (2006) 12–19.
[18] C.Y. Miao, G. Lu, Y.W. Yao, G.Y. Tang, D. Weng, J.H. Qiu, M. Mizuno, Chem. Lett. 36 (2007) 494–495.
[19] X.X. Zhang, X.C. Wang, X.M. Tao, K.L. Yick, J. Mater. Sci. 40 (2005) 3729–3734.
[21] X.X. Zhang, Y.F. Fan, X.M. Tao, K.L. Yick, Mater. Chem. Phys. 88 (2004) 300–307.
[22] W. Li, X.X. Zhang, X.C. Wang, J.J. Niu, Mater. Chem. Phys. 106 (2007) 437–442.
[23] C. Alkan, A. Sari, A. Karaipekli, Sol. Energy Mater. Sol. Cells 93 (2009) 143–147.
[24] X.X. Zhang, X.M. Tao, K.L. Yick, X.C. Wang, Colloid Polym. Sci. 88 (2004) 330–337.
[25] Y. Yamagishi, S. Tomohisa, I. Takashi, Proceeding of the Intersociety Energy Conversion Engineering Conference, vol. 3, 1996, pp. 2077–2081.
[26] R. Ludwig, V.O. Clinton, F.K. Laurence, Text. Res. J. 41 (1971) 139–146.